

Hydrogen H α line polarization in solar flares

Theoretical investigation of atomic polarization by proton beams considering self-consistent NLTE polarized radiative transfer

J. Štěpán^{1,2}, P. Heinzel¹, and S. Sahal-Bréchet²

¹ Astronomical Institute, Academy of Sciences of the Czech Republic, Fričova 298, 251 65 Ondřejov, Czech Republic
e-mail: [stepan;pheinzel]@asu.cas.cz

² LERMA, Observatoire de Paris – Meudon, CNRS UMR 8112, 5, place Jules Janssen, 92195 Meudon Cedex, France
e-mail: [jiri.stepan;sylvie.sahal-brechot]@obspm.fr

Received 1 September 2006 / Accepted 20 December 2006

ABSTRACT

Context. We present a theoretical review of the effect of impact polarization of a hydrogen H α line due to an expected proton beam bombardment in solar flares.

Aims. Several observations indicate the presence of the linear polarization of the hydrogen H α line observed near the solar limb above 5 % and preferentially in the radial direction. We theoretically review the problem of deceleration of the beam originating in the coronal reconnection site due to its interaction with the chromospheric plasma, and describe the formalism of the density matrix used in our description of the atomic processes and the treatment of collisional rates.

Methods. We solve the self-consistent NLTE radiation transfer problem for the particular semiempirical chromosphere models for both intensity and linear polarization components of the radiation field.

Results. In contrast to recent calculations, our results show that the energy distribution of the proton beam at H α formation levels and depolarizing collisions by background electrons and protons cause a significant reduction of the effect below 0.1 %. The radiation transfer solution shows that tangential resonance-scattering polarization dominates over the impact polarization effect in all considered models.

Conclusions. In the models studied, proton beams are unlikely to be a satisfying explanation for the observed linear polarization of the H α line.

Key words. Sun: flares – polarization – atomic processes – radiative transfer – line: formation

1. Introduction

Observations of solar flares in the hard X-ray spectral region indicate a non-thermal origin of this radiation (Frost 1969). There are several mechanisms that can be identified as a possible source of this emission (Korchak 1967). Presently, there is wide consensus among solar physicists that the most likely explanation is the bremsstrahlung radiation of electron beams with energies of the order 10–100 keV, which are injected into denser layers of the solar atmosphere from a coronal reconnection site. The differential energy spectrum of these beams at the injection site is usually assumed to have a power-law distribution $\sim E^{-\delta}$ with δ between 3 and 5 (Brown 1971).

Although there is also observational evidence of high energetic protons (above 10 MeV) in the γ -ray spectrum, radiation induced by protons at energies below 1 MeV is difficult to detect because they do not radiate efficiently at such energies. Several processes that lead to electron acceleration at the reconnection site can also lead to acceleration of protons (see Orrall & Zirker 1976, and references therein). The existence of low energy proton beams in solar flares is still uncertain, but it is believed that they may also play a significant role in flare physics. Furthermore, energetic electron beams cannot be used as a satisfactory explanation for all flare observations (e.g., Doschek et al. 1996). For

a comparison of the effects of electron and proton beams see Brown et al. (1990).

There are several techniques that can be used to detect low energy proton beams. The emission peak in the H α core due to proton beam bombardment was proposed by Hénoux et al. (1993). It has been recently shown by Xu et al. (2005a) that this effect does not exist. Another technique is based on measurements of the red-shifted emission in line wings, especially in the hydrogen Ly α line, which is a consequence of the charge exchange effect (Orrall & Zirker 1976; Canfield & Chang 1985; Brosius et al. 1995; Fang et al. 1995; Zhao et al. 1998; Brosius & Woodgate 1999). A different approach is based on the fact that anisotropic excitation of the chromosphere atoms by a directed proton (or electron) beam induces a preferential population of particular Zeeman sublevels, i.e., the impact atomic polarization and, consequently, an emission of linearly polarized radiation (Hénoux et al. 1990).

Some observations indicate the existence of linear polarization of the H α line in solar flares above 5 % or even as high as 10 % (Hénoux & Chambe 1990; Vogt & Hénoux 1996; Xu et al. 2005b) and preferentially oriented towards the disk center (it will be denoted as *radial* in this paper) and also parallel to the limb (i.e., *tangential*). This effect is usually interpreted as a consequence of the impact polarization by a vertical proton beam with energy below 200 keV in the H α core forming layers.

Contrary to these measurements, there are observations that indicate no linear polarization in a wide range of flares (Bianda et al. 2005) and argue for isotropization of the beam at crucial atmospheric depths. Studies of H α polarization in solar prominences show that transitions between fine structure levels within the shell $n = 3$ of hydrogen caused by collisions with background electrons and protons lead to a significant depolarizing effect (Bommier et al. 1986b) even at densities of the order of 10^{10} cm^{-3} . The electron (proton) density in a flaring solar chromosphere at the H α formation levels is above 10^{12} cm^{-3} , therefore this effect could significantly reduce measurable polarization.

In recent years, a first quantitative estimation of the hydrogen impact polarization under the flare conditions has been done by Vogt et al. (1997) and Vogt et al. (2001). In these calculations, a self-consistent radiative transfer code for unpolarized radiation has been used to find the hydrogen ionization degree and the radiation intensity at unit optical depth of H α for several semiempirical atmospheric models and under the effect of proton beams having several parameters. In these calculations, the following approximation has been used: The equations of statistical equilibrium and the radiation transfer equations have been decoupled and the H α line has been assumed to be optically thin. The proton beam energy distribution at an injection site has been assumed to be similar to the one deduced for electron beams, i.e., a power law. The lower energy cut-off E_c is usually set between 100 to 200 keV. This energy approximately corresponds to the energy necessary for a proton to reach the H α line-forming layers. Using an assumption that the power-law distribution preserves its character while the beam propagates to the upper chromosphere, these authors calculated the polarization degree of emitted radiation. Depolarization by collisions with electrons and protons of the ambient medium have also been taken into account. Depending on the atmosphere model and beam parameters, the predicted polarization degree has been up to 4.5 %. However, a complete solution of the coupling of the polarized radiative transfer to the atomic equilibrium has not been tackled.

The aim of this paper is to present a theoretical analysis of the proton impact polarization phenomenon in the hydrogen H α line based on NLTE polarized radiative transfer. Our goal is to verify the assumption that the measured linear polarization can be interpreted as due to this mechanism. In particular, we have focused our attention to a limiting case of unidirectional non-deflecting beams, which are supposed to generate highest polarization due to their extremal anisotropy. For simplicity we use a static 1D model of the flaring chromosphere.

In the second section, the deceleration effect of the chromosphere on proton beams is reviewed and some conclusions are made about the low-energy beam fluxes in H α -forming layers. These are compared with the assumptions made in the previous works. The third section describes our NLTE solution of the unpolarized transfer in an atmosphere affected by non-thermal excitation and ionization by proton beam. This solution is similar to that of Kašparová & Heinzel (2002), which has been performed for electron beams. We use the same approach to calculate the volume densities of thermal electrons and protons in the chromosphere. These densities are then used in our polarized transfer code. After that we describe the framework of the quantum density matrix and equations of atomic statistical equilibrium on the basis of irreducible tensorial operators. The fifth section is dedicated to the problem of collisional rates for all transitions used in our modeling. Sect. 6 contains a comparison of results obtained by Vogt et al. (2001) with our calculations in the last scattering approximation. A brief description of po-

larized transfer solution and the method used in our calculations can be found in Sect. 7. The results and their discussion are summarized in Sect. 8. In the last section our conclusions are made and the main consequences for the interpretation of observations are pointed out. All expressions in this paper are written using the CGS system of units.

2. Solar atmosphere models and beam propagation

2.1. Proton beam propagation

Let us briefly review the interaction of a proton beam with the solar chromosphere. We assume a beam in the coronal reconnection site, which vertically penetrates the chromosphere. A horizontal motion of the protons is neglected to obtain as anisotropic a velocity distribution as possible. The energy of protons necessary to reach the H α formation levels is of the order of 100 keV at the top of the chromosphere (see below). Protons of such high energy do not lose a lot of energy in the interaction with extremely hot coronal plasma (Hénoux et al. 1993), hence we may neglect any interaction with the coronal mass in this paper. In all our calculations, the energy of the superthermal protons ($> 1 \text{ keV}$) of the beam is high above the average energy of thermal motions in the chromosphere where H α is formed, thus we can use the so-called cold target approximation (Emslie 1978).

In a partially ionized medium, a superthermal proton beam is decelerated by collisions with the background electrons and ions and also by elastic and inelastic collisions with neutral atoms, especially the atmosphere's main constituent, hydrogen. We will use the approach of Emslie (1978) to describe this deceleration and the beam energy deposition into the atmosphere. The deceleration by charged electrons and protons can be quantified by means of the Coulomb logarithm Λ . The inelastic and elastic scattering on the neutral hydrogen is similarly described by Λ' and Λ'' , respectively. These logarithms vary slightly according to atmospheric properties, but these changes are small within a wide range of physical characteristics and it will not affect our results significantly if we suppose these quantities to be constant. The values adopted in this paper have been set according to typical physical properties of the upper chromosphere: $\Lambda = 23$, $\Lambda' = 3$. Elastic scattering of the proton beam on neutral hydrogen is negligible in comparison to other processes and will be neglected.

Let $F(E, N)$ be the energy distribution of the number flux of beam particles at the column depth N . At the injection level we set $N = 0$. The general form of this distribution is (Canfield & Chang 1985)

$$F(E, N) = F(\sqrt{E^2 + E_N^2}, 0) \frac{E}{\sqrt{E^2 + E_N^2}}. \quad (1)$$

For the purposes of our calculations, we have used an initial power-law energy distribution at the injection site, which is usually considered in the non-thermal flare heating problems (Brown 1971)

$$F(E, 0) = (\delta - 2)E_c^{\delta-2} \mathcal{E}_0 E^{-\delta} \theta(E - E_c), \quad (2)$$

where

$$\theta(x) = \begin{cases} 1 & (x > 0) \\ 0 & (x < 0) \end{cases} \quad (3)$$

is the Heaviside function, E_c is the lower energy cut-off of the distribution, and \mathcal{E}_0 is the total initial energy flux of the beam.

E_c is usually assumed to lie between 100 keV and 200 keV, according to minimal energy necessary for protons to reach the H α formation layers. The formula (1) for the particular case of initial distribution (2) gives (Zhao et al. 1998)

$$F(E, N) = (\delta - 2)E_c^{\delta-2}\mathcal{E}_0 \frac{E}{(E^2 + E_N^2)^{\frac{\delta+1}{2}}}, \text{ for } E \geq E_m, \quad (4)$$

where

$$E_m(N) = \begin{cases} \sqrt{E_c^2 - E_N^2}, & (E_N \leq E_c) \\ 0, & (E_N > E_c) \end{cases} \quad (5)$$

is the minimum energy of the distribution at a given depth.

The energy deposition rate into the neutral hydrogen is given by

$$I_{H1}(N) = \frac{Kn_H}{2}(\delta - 2)(1 - x)\Lambda' \frac{m_p}{m_e} \frac{\mathcal{E}_0}{E_c^2} \left(\frac{N}{N_c}\right)^{-\frac{\delta}{2}} B_{x_c}\left(\frac{\delta}{2}, \frac{1}{2}\right), \quad (6)$$

where

$$x_c = \begin{cases} N/N_c, & (N < N_c) \\ 1, & (N > N_c) \end{cases}, \quad (7)$$

and $B_x(a, b)$ is the incomplete beta function. N_c is the depth that can be reached by protons with the initial energy E_c . Eq. (6) is a special case of the Eq. (1) of Kašparová & Heinzel (2002), here for a non-deflecting vertical proton beam. This energy deposition rate has been used in calculations of the ionization degree of the chromosphere described in Sect. 3.

2.2. Flux distribution at H α formation level

The distribution (4) has been plotted in Fig. 1 for several values of E_N , typical energy cut-off $E_c = 150$ keV and two initial spectral indices δ . The first fact that should be pointed out is that the energy cut-off does not significantly depend on E_N if $E_N < E_c$ until $E_N \approx E_c$. It is because high energy protons are decelerated inefficiently. Only if $E_N \rightarrow E_c$, protons are slowed to energies close to 5 keV¹. Using Eq. (4) we find that the flux of the beam at the local energy cut-off E_m is lower by factor $(E_c/E_N)^\delta E_m/E_N$ compared to the flux $F(E_c, 0)$. Hence we have a strong decrease of flux close to the interesting energy range (i.e., $E_m \ll E_c$) by the factor of approximately E_m/E_c . The total flux is rapidly reduced in deeper layers ($E_N > E_c$). It can be shown that the flux maximum is at the energy $E_N/\sqrt{\delta}$. After crossing some critical depth, the flux of the beam with lower δ dominates the one with higher δ at all energies – because initially there is a higher number of high energy protons in the small- δ case, which are now decelerated to low energies. As a result, energy is more effectively deposited by small- δ beams in lower depths, while high- δ beams are decelerated in upper layers. In any case, the decrease of flux $\partial F(E, E_N)/\partial E_N$ is steep for any δ and one could expect that impact polarization will be sensitive to the E_c value because there is only a small ΔE_N interval in which low-energy flux is not negligible, and this depth interval should overlap with the H α line center formation region as much as possible. It is not possible to have a power-law-like distribution at this layer with a local cut-off of about 5 keV for beams starting at the top of chromosphere with energies above 100 keV or higher.

This leads us to the second conclusion. The energy distribution of the flux cannot be approximated by the power-law

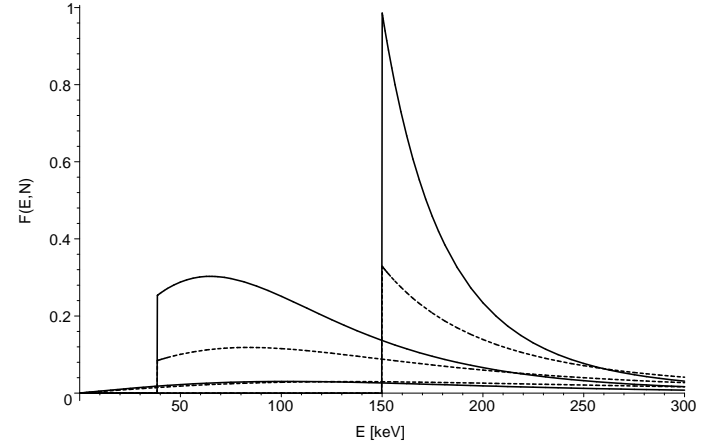


Fig. 1. Energy distribution of the beam with initial energy cut-off $E_c = 150$ keV at depths with different E_N . Solid curves correspond to spectral index $\delta = 5$, dashed curves to $\delta = 3$. From upper to lower, the curves are plotted for $E_N = 0, 145$ and 230 keV. The cut-off energy at depths close to N_c is still of the order of E_c . At deeper depths the distribution $\delta = 3$ dominates over $\delta = 5$ at all energies.

curve if E_N is close to E_c . If these energies are comparable (and that is the case of our interest here because we have for maximum impact polarization $E_c \approx 5$ keV $\ll E_c$), the use of the power-law distribution leads to an unrealistic overestimation of the polarization degree. Such an approximation has been used by Vogt et al. (1997) and by Vogt et al. (2001) with lower energy cut-off varied from 1 keV to 20 keV and with a total beam number flux and δ conserved. The theoretical values of polarization obtained from these calculations should therefore be revised.

3. Unpolarized radiation modeling and background electron and proton densities

Our solution of unpolarized radiation transfer follows the approach of Hénoux et al. (1993) and Kašparová & Heinzel (2002). We take a 1D static atmosphere with fixed temperature structure and other plasma properties given by the semiempirical chromosphere model of the flaring atmosphere F1 (Machado et al. 1980), and following Vogt et al. (1997) and Vogt et al. (2001) we also use the model VAL F (Vernazza et al. 1981) for comparison. These models have been created using a number of line and continuum observations.

The non-thermal proton beam dissipates its energy while propagating through the matter of the chromosphere causing its heating and the modification of atomic level populations and ionization. The non-thermal heating is already included in the semiempirical flare models to explain the observed emission. Our approach to the modeling follows the approach of Hénoux et al. (1993) and Kašparová & Heinzel (2002). We consider a fixed temperature structure of the atmosphere as given by the semiempirical atmosphere models. The pressure and statistical equilibrium equations are solved together with radiation transfer. Then we study an influence of the non-thermal collisional rates on the line profiles in comparison to the thermal model (differential approach). It is important to notice that the temperature of the flaring atmosphere described by semiempirical models is in general overestimated because it has been determined to explain the increased radiation emission regardless of the non-thermal excitation and ionization. The same approach

¹ As we will show later, the low-energy protons (4–5 keV) are most effective in producing impact polarization of $n = 3$ hydrogen level.

has been used for the solution of the polarized radiative transfer (Sect. 7) to obtain the changes of the H α Q/I -profiles after introduction of the non-thermal collisional rates into statistical equilibrium equations. The only difference is that the polarized solution uses the electron and proton densities precalculated by the unpolarized transfer code. We have used the same MALI code as Kašparová & Heinzel (2002), now adapted to treat proton beam bombardment described in Sect. 2. The code has been run with a four-level plus continuum hydrogen atomic model and non-thermal collisional rates have been calculated from the energy deposition rate into hydrogen (6) using the expressions (10) and (11) of Hénoux et al. (1993).

The electron densities (which are close to proton densities at H α core formation layers) are plotted in Figs. 2 and 3 for both models under consideration, several beam fluxes, and three different values of δ . These calculations show that ambient electron (and proton) densities used by Vogt et al. (1997) are underestimated (cf. Tables 2 and 3 therein) and the same is true for the mean radiation intensities. These values have been computed in the layers of total (coronal + chromospheric above H α -forming layers) column mass depth $2.484 \times 10^{-4} \text{ g cm}^{-2}$ (VAL F, see Table 15 of Vernazza et al. 1981) and $3.186 \times 10^{-4} \text{ g cm}^{-2}$ (F1, see Table 3 of Machado et al. 1980), where the optical depth of H α is approximately unity. Because our background particle densities did not correspond to the ones presented by Vogt et al. (1997), we have used their radiation transfer code which is based on the standard Λ -iteration process. We have found that this code setting (the accuracy of 10^{-3} in maximum relative change of atomic populations between subsequent iterations) leads to insufficient convergence and consequently to the underestimation of electron and proton densities. An increase of accuracy led to values close to ours, but at the cost of an extremely large number of Λ -iterations (for similar tests see also Kašparová & Heinzel 2002).

In Fig. 4 one can see the theoretical H α line profile for the same beam fluxes as in Fig. 2. These profiles are consistent with the results of Xu et al. (2005a). In comparison to profiles presented by Hénoux et al. (1993), the central emission in the line core does not appear.

4. Formalism of density matrix and local equilibrium

The electron densities in the layers of interest do not exceed 10^{13} cm^{-3} . Following Bommier & Sahal-Br  chot (1982) and Bommier et al. (1986a), the hyperfine splitting of the hydrogen levels is completely negligible. In fact the hyperfine splitting of the relatively long-living $3s^{1/2}$ level (about 50 MHz) is higher than its inverse radiative lifetime (of the order of 1 MHz) and thus the hyperfine levels do not overlap. However, it was verified by Bommier et al. (1986a) that taking the hyperfine structure into account does not affect the linear polarization of the Balmer lines in any significant way. Moreover, in the conditions under consideration, the lifetimes of the levels are strongly reduced by collisions with the charged perturbbers. The lifetimes of the $n = 3$ levels are of the order of a few 100 MHz in the H α core-forming layers due to the dipolar transitions $nlj \rightarrow nl \pm 1j'$ (cf. Sahal-Br  chot et al. 1996); hence, much greater than hyperfine splitting. Therefore, we take into account only the fine structure splitting of the levels. We suppose that there are no quantum coherences between different energy levels. This assumption is valid in our model of the hydrogen atom where the individual level widths are smaller than distances between them or where the selection rules for dipolar optical transitions prevent creation

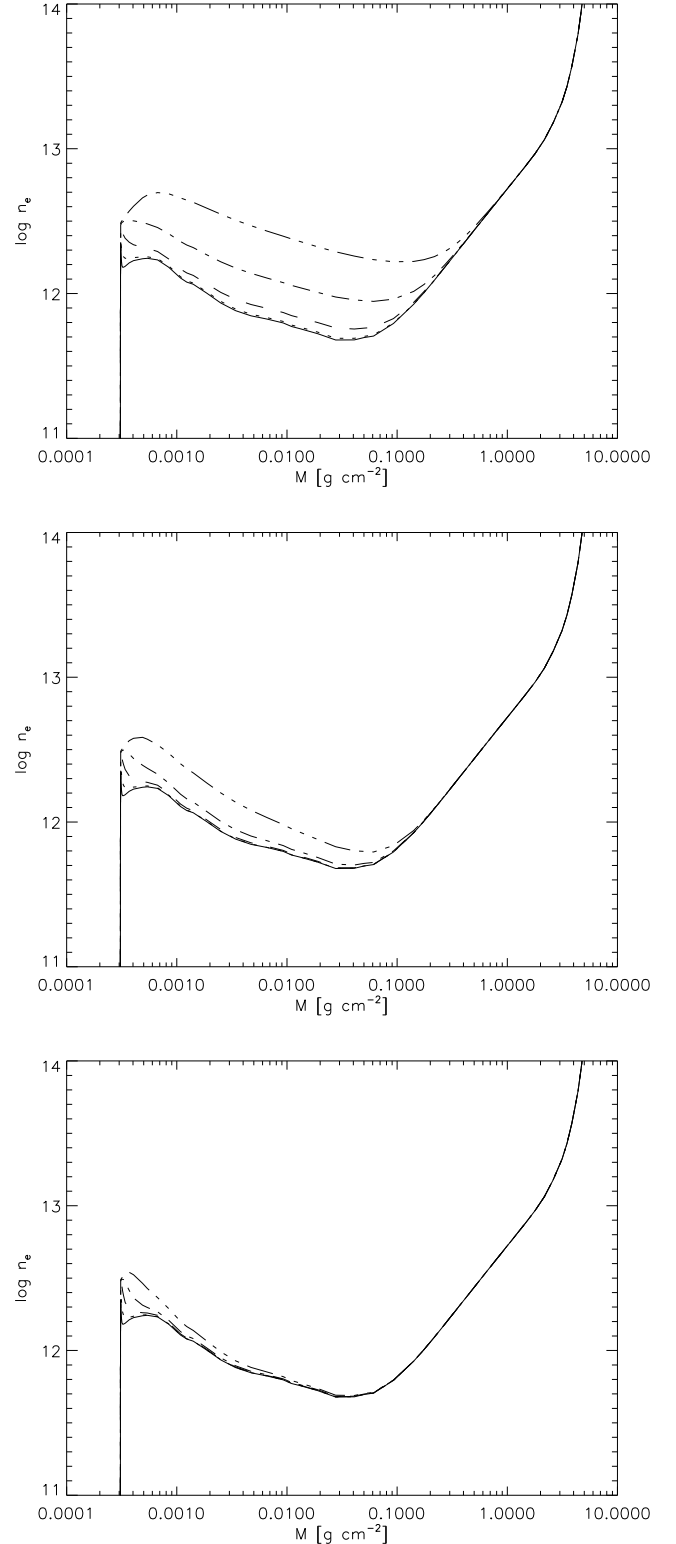


Fig. 2. Electron density for the model F1. The plots correspond to the case $\delta = 3$ (upper panel), $\delta = 4$ (middle panel), and $\delta = 5$ (lower panel). The thermal case is plotted by a solid line, the non-thermal beam fluxes are $E_0 = 10^8$ (dot), 10^9 (dash), 10^{10} (dash-dot), and $10^{11} \text{ erg cm}^{-2} \text{ s}^{-1}$ (dash-dots). All beams have $E_c = 150 \text{ keV}$.

of coherences. As a result, the fine structure levels are supposed to be completely separated.

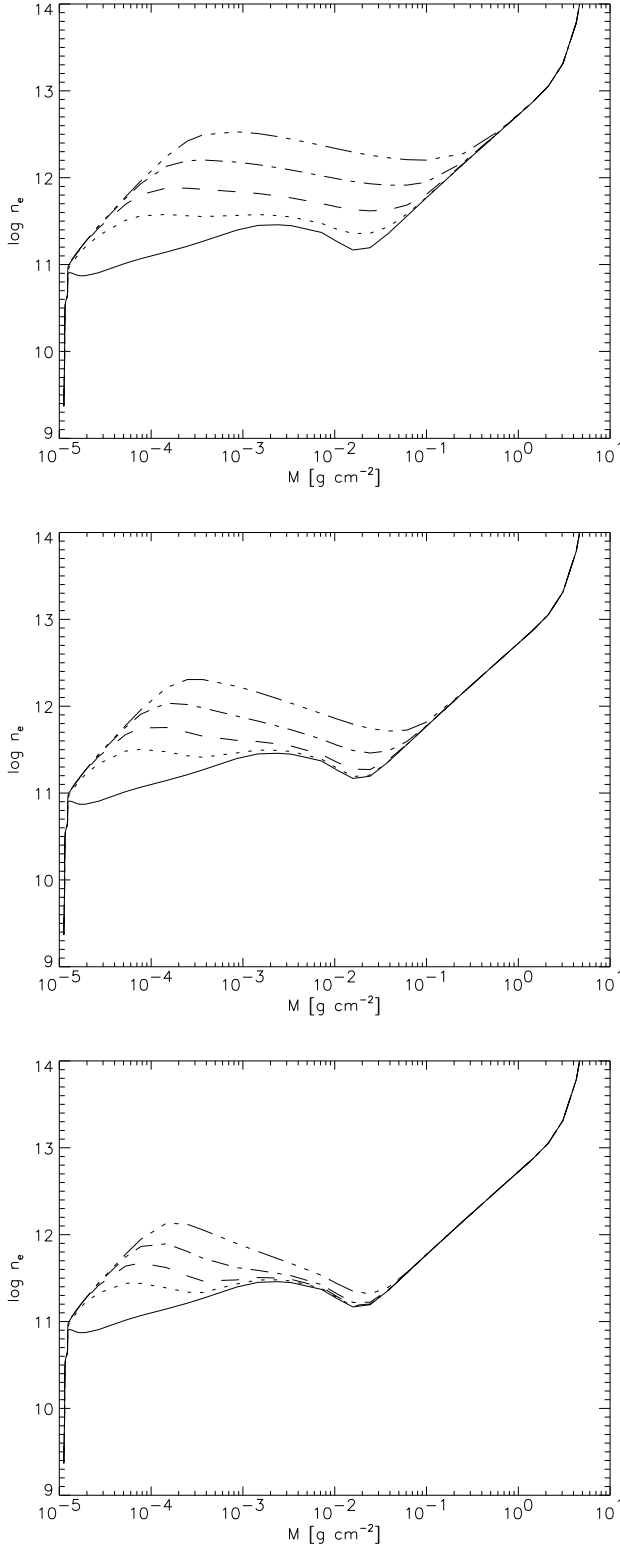


Fig. 3. Same as Fig. 2; here for the VAL F model.

To describe the state of hydrogen atoms in an equilibrium with the radiation field and charged colliders, we adopt the framework of the atomic density matrix ρ (e.g., Fano 1957). In the dyadic basis $|nljm\rangle$ of hydrogen states, we adopt the common notation: n is the principal quantum number, l the orbital one, and j is the total angular momentum. Magnetic quantum number

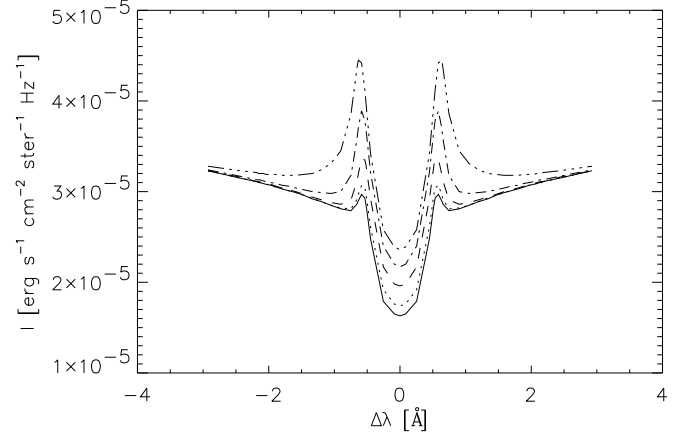


Fig. 4. H α line profiles for the model F1 and $\delta = 4$. The particular profiles correspond to the same beam fluxes as in Fig. 2.

is represented by m . The natural basis for the density matrix operator in polarization studies is that of irreducible tensorial operators (ITO or the multipole expansion) T_q^k (Sahal-Br  chot 1977). In all our development we suppose that all the particle velocity distributions and the radiation field are axially symmetric with the symmetry axis in a vertical direction. We also assume that the magnetic field lines are oriented along the vertical axis and that the strength of the magnetic field is at most a few hundred gauss (thus we can neglect the Zeeman splitting of the levels). All of these assumptions lead to a great simplification of calculations because most of the density matrix elements vanish: All the coherences between the wave functions of the states vanish. In the basis of ITO only the components ρ_{nlj}^k remain. These diagonal elements represent population ($k = 0$) and alignment ($k = 2$) components of the different levels. Again, due to symmetry reasons ($\rho_{nljm} = \rho_{nlj-m}$), the elements with odd k vanish. One could take into account the anti-level-crossing effect (Bommier 1980) related to the so-called alignment-to-orientation mechanism (cf. Landi Degl’Innocenti 1982), which can lead to creation of some non-zero density matrix components of odd rank (so-called orientation), even if no circularly polarized radiation is present. In fact, this effect is of little importance in our current model because the magnitude of the created orientation remains well below the magnitude of the alignment. Therefore we can safely exclude this effect from our study. The higher multipoles ($k > 2$) do not affect the solution under given the physical conditions and they have been neglected.² We limit our analysis to the three principals levels of the hydrogen atom.

Our calculations concern a static model. The local hydrogen equilibrium is expressed by the equations of statistical equilibrium (ESE)

$$\Pi\rho = u. \quad (8)$$

The elements of matrix Π consist (in the impact approximation) of the collisional and radiative rates simply summed together: $\Pi_{nlj \rightarrow n'l'j'}^{k \rightarrow k'} = R_{nlj \rightarrow n'l'j'}^{k \rightarrow k'} + C_{nlj \rightarrow n'l'j'}^{k \rightarrow k'}$ (Bommier & Sahal-Br  chot 1991). The diagonal elements in $nlj \equiv n'l'j'$ stand for relaxation of the level nlj to another levels, while the nondiagonal elements stand for populating a given multipole component. The

² The only non-zero multipole $k \geq 4$ in the third-principal level hydrogen is $3d\frac{5}{2}\rho_0^4$ and one has $3d\frac{5}{2}\rho_0^4 \ll 3d\frac{5}{2}\rho_0^2 \ll 3d\frac{5}{2}\rho_0^0$.

relaxation rates will be marked by the index “R” in this paper. The detailed analysis of the structure of Π can be found in Sahal-Br  chot (1977). ρ is the formal vector of density matrix components $^{nlj}p_0^k$. The normalization condition on the density matrix has to be introduced: The sum of all level populations is equal to 1. We know that the relative population of level nlj is equal to $\sqrt{2j+1}^{nlj}p_0^0$, and hence we may replace the first row of Π by the appropriate constant elements and the right-hand-side of Eq. (8) reads $u = (1, 0, \dots, 0)^T$.

The particular expressions for the R -matrix elements can be found in Landi Degl’Innocenti (1984). They are calculated in the lowest order of quantum electrodynamics from a known radiation field. Only the single events of emission and absorption are considered. We adopt the approximation that there is no coherence between the frequency of absorbed and emitted photons. This approximation is known as a complete frequency redistribution (CRD; cf. also Sect. 7). The elements of the matrix of collisional rates C can be calculated taking into account several collisional processes as will be described in the following section.

5. Collisional rates in detail

First of all we stress that we limit our analysis of collisional transitions to density matrix multipoles of $k = 0$ and $k = 2$. Higher ranks do not significantly affect polarization in the studied problem and will be neglected. Collisional rates $C_{nlj \rightarrow n'l'j'}^{k \rightarrow k'}$ and $R_{nlj \rightarrow n'l'j'}^{k \rightarrow k'}$ of hydrogen can be calculated from cross-sections $\sigma_{nlj \rightarrow n'l'j'}^{k \rightarrow k'}(v)$ of appropriate transitions by integration over the relative velocity distribution $f(v)$ of particles

$$C_{nlj \rightarrow n'l'j'}^{k \rightarrow k'} = N_P \int d^3v f(v) v \sigma_{nlj \rightarrow n'l'j'}^{k \rightarrow k'}(v), \quad (9)$$

and similarly for relaxation rates. N_P stands for the perturbers volume density.

The processes taken into account in our analysis are the following:

1. Fine structure dipole transitions induced by ambient electrons $e^- + (H I)^{nlj} \rightarrow e^- + (H I)^{n\pm 1j'}$.
2. Fine structure dipole transitions induced by ambient protons $p^+ + (H I)^{nlj} \rightarrow p^+ + (H I)^{n\pm 1j'}$.
3. (De)excitation by ambient electrons $e^- + (H I)^{nlj} \rightarrow e^- + (H I)^{n'l'j'}$.
4. Excitation by proton beam $p_B^+ + H I \rightarrow p_B^+ + (H I)^*$.
5. Charge exchange excitation $p_B^+ + H I \rightarrow (H I)_B^* + p^+$.

The index “B” is reserved for particles of the beam and an asterisk (*) is used for an excited state of the neutral hydrogen H I. p^+ and e^- denote protons and electrons, respectively. The other possible collisional transitions have been neglected due to their negligible effect. The cross-sections of these processes have been obtained in several ways.

The fine structure transitions within the same shell ($nlj \rightarrow n'l \pm 1j'$) have been calculated using the semiclassical perturbation method (Sahal-Br  chot et al. 1996). This approach is accurate for calculation of transitions between close levels (in comparison to collision energy) in a dipolar approximation. Using the formalism of the previously referenced paper, rates can be expressed in the form

$$C_{nlj \rightarrow n'l'j'}^{k \rightarrow k'} = N_P \left(\delta_{kk'} c_{k,j \rightarrow j'}^{(0)} \alpha_{nlj \rightarrow n'l'j'}^{(0)} \right.$$

$$\left. + c_{k \rightarrow k',j \rightarrow j'}^{(2)} \alpha_{nlj \rightarrow n'l'j'}^{(2)} \right), \quad (10)$$

$$R_{nlj \rightarrow n'l'j'}^{k \rightarrow k'} = N_P \left(\delta_{kk'} R_{k,j \rightarrow j'}^{(0)} \alpha_{nlj \rightarrow n'l'j'}^{(0)} \right. \\ \left. + R_{k \rightarrow k',j \rightarrow j'}^{(2)} \alpha_{nlj \rightarrow n'l'j'}^{(2)} \right), \quad (11)$$

with

$$\alpha_{nlj \rightarrow n'l'j'}^{(0)} = \sqrt{4\pi} \int_0^\infty \sigma_{nlj \rightarrow n'l'j'}^{(0)}(v) f_0(v) v^3 dv, \quad (12)$$

$$\alpha_{nlj \rightarrow n'l'j'}^{(2)} = \sqrt{\frac{4\pi}{5}} \int_0^\infty \sigma_{nlj \rightarrow n'l'j'}^{(2)}(v) f_2(v) v^3 dv. \quad (13)$$

The cross sections $\sigma_{nlj \rightarrow n'l'j'}^k$ have been defined by expressions (59) and (60) of the referenced paper. f_0 and f_2 are the monopole and quadrupole components of the relative velocity distribution with axial symmetry. The angular coefficients c have been defined by expressions (66)–(69) of Sahal-Br  chot et al. (1996). Although this method is limited only to treatment of dipolar transitions $l \rightarrow l \pm 1$, these transitions are dominant in the important range of collisional energies at chromospheric temperatures.

Excitation transition probabilities from the ground state $1s \frac{1}{2}$ to upper levels induced by thermal electrons have been calculated using the cross-section data of database AMDIS.³ These data are provided for $1s \rightarrow nl$ transitions neglecting the fine structure of the levels, and therefore we use an approximation by the angular coefficient to obtain the fine structure cross-sections (Vogt et al. 2001).

$$\sigma_{1s \frac{1}{2} \rightarrow nlj}^{0 \rightarrow k} = (-1)^{j+l+k+\frac{1}{2}} \frac{2j+1}{\sqrt{2}} \left\{ \begin{matrix} l & l & k \\ j & j & \frac{1}{2} \end{matrix} \right\} \sigma_{1s \rightarrow nl}^{0 \rightarrow k}. \quad (14)$$

At the present time, we do not have any adequate cross-section data for the fine structure transitions between levels $n = 2$ and $n = 3$. Therefore we have calculated these cross sections using the same semiclassical perturbation method, although these cross sections are overestimated and cannot be used for non-dipolar transitions $2s \rightarrow 3d$.

The cross sections of direct excitation to levels $n = 2$ and $n = 3$ by protons have been calculated using the data of Balan  a & Feautrier (1998). These authors give cross sections $\sigma_{1s \rightarrow nl}^{0 \rightarrow k}$ for population and alignment excitation in the energy range of 1 keV to 100 keV. As well as in the case of excitation by thermal electrons, we use the expression (14) to obtain data for the fine structure transitions. The transitions $n = 2 \rightarrow n = 3$ have been neglected. The self-consistent solution of radiation transfer requires us to know the cross sections at energies above 100 keV. This is due to the behavior of the energy distribution of proton beams at different depths. Although the total flux of the beam decreases quickly as the depth exceeds N_c , the role of high energy protons increases: the maximum of the distribution $F(E, N > N_c)$ is at the energy $E_N / \sqrt{\delta}$. This leads to the emission in the near H α line wings and neglecting these energies leads to unrealistic line profiles. We have used the semiclassical perturbation method to calculate dipolar cross sections at energies above 100 keV. The transitions $1s \rightarrow 3d$ cannot be calculated by this method, and therefore we used a similar approximation as Vogt et al. (1997) and set these transitions to one tenth of the value of $1s \rightarrow 3p$ cross-sections. This approximation is based on the observation that the electron cross-sections for $1s \rightarrow 3d$ excitation are approximately 1/10 of $1s \rightarrow 3p$ at high energies

³ Atomic and Molecular Data Information System, <http://www-amdis.iaea.org/>

(Aboudarham et al. 1992), and it is also true for 100 keV protons (Balança & Feautrier 1998). While this is not fully justifiable, it should improve accuracy of the solution.

The effect of the charge exchange has also been taken into account using the data of Balança & Feautrier (1998). On the one hand this process is efficient at energies around 25 keV, on the other hand its cross section decreases fast at higher energies. A more detailed analysis of the effect of the charge exchange and the associated Doppler shift of the line can be found in Sect. 7. Contrary to direct excitation, no approximation of the cross-sections at energies above 100 keV has been used. These cross-sections can be safely neglected due to their small magnitude.

6. Impact polarization without polarized transfer

In this section, we will compare several results of atomic impact polarization obtained by Vogt et al. (2001) with our calculations performed by a similar method. We will consider the emission of radiation under the proton beam bombardment in chromospheric conditions. The local atmosphere conditions (temperature, thermal electron and proton densities, and mean radiation intensity in the hydrogen L α , L β , and H α lines) are obtained from the unpolarized radiative transfer solution. These conditions are taken at unit H α line center optical depth. Following Vogt et al. (1997, 2001) we assume that proton beam energy distribution is given by a power law with the same spectral index δ as at the injection coronal site. The emitted radiation, which is polarized due to beam impacts, is assumed to be unaffected by radiation transfer in upper layers in this approach. Although a rough approximation, it can serve as a comparison of our calculation of collisional rates and local equilibrium, which will be used in further self-consistent solutions.

After calculation of the density matrix elements from Eq. (8) one can calculate the ratio ϵ_Q/ϵ_I of emission coefficients of the Stokes parameters Q and I . When observed at solar limb (i.e., 90 degrees from the vertical direction) and through the optically thin layer, this ratio could provide an estimation of the emergent light polarization degree. From known atomic density matrix elements, the polarization of emergent radiation reads

$$p_{90}(n \rightarrow n') = -\frac{3\vartheta_{n \rightarrow n'}^{(2)}}{2\sqrt{2}\vartheta_{n \rightarrow n'}^{(0)} - \vartheta_{n \rightarrow n'}^{(2)}}, \quad (15)$$

with

$$\vartheta_{n \rightarrow n'}^{(k)} = \sum_{ll'jj'} (-1)^{1+j+j'} (2j+1) A_{nlj \rightarrow n'l'j'} \left\{ \begin{matrix} j & j & k \\ 1 & 1 & j' \end{matrix} \right\} n l j \rho_0^k. \quad (16)$$

The quantity $A_{nlj \rightarrow n'l'j'}$ is the Einstein coefficient for spontaneous emission and the entities in the braces are the so-called 6j symbols. At the level of unit H α optical depth, the beam energy cutoff is, by definition, close to zero. This cutoff has been varied in the interval 1 keV to 20 keV by Vogt et al. (2001) to find the dependence of the polarization degree. These authors show that the polarization degree can be expected as high as 2.5 % for model VAL F and 0.7 % for model F1 ($\delta = 4$), or 5 % for model VAL F and 1.2 % for model F1 ($\delta = 5$). The results of Vogt et al. (2001) contained in their Table 1 are plotted in Fig. 5.

We have repeated these calculations for the same conditions, with $E_c(\tau_{H\alpha} = 1)$ varied between 1 keV and 20 keV and total initial beam energy flux between 10^8 to 10^{11} erg s $^{-1}$ cm $^{-2}$. The physical conditions of the atmosphere have been taken from

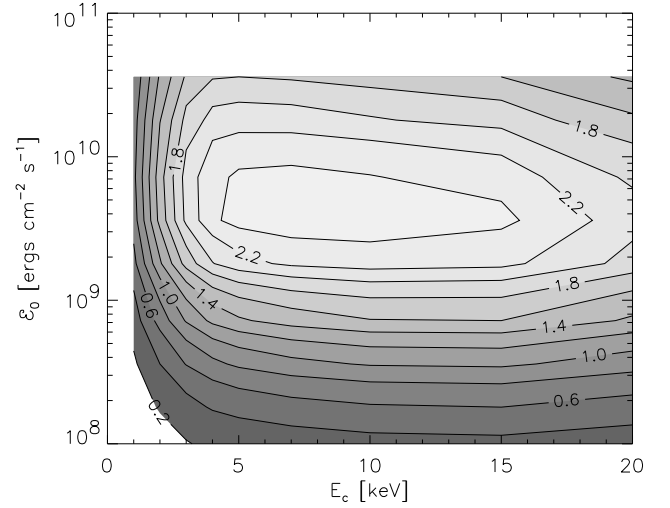


Fig. 5. Emergent polarization degree (in percent) of the on-limb observation calculated by Vogt et al. (2001) in the last scattering approximation. The horizontal axis shows the value of the local energy cut-off, and the vertical axis shows the values of the initial beam flux.

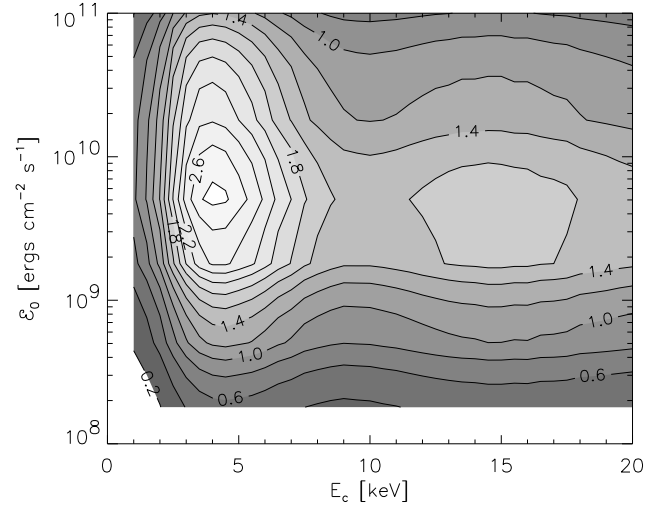


Fig. 6. Same as Fig. 5; here calculated using another numerical integration technique and different cross-section data for the electron excitation (see text for details).

Tables 2 and 3 of Vogt et al. (1997). The corresponding polarization degree for VAL F model is plotted in Fig. 6.

Although the order of both results agrees, there are differences between these solutions. The most important difference is a steeper decrease of polarization degree at higher energies. The reasons for these differences are the different cross-sections used for electron–hydrogen excitation and especially the different technique of numerical integration used for calculation of non-thermal collisional rates. While the Gauss-Laguerre quadrature has been used in Vogt’s calculations, we have chosen an adaptive Simpson rule with a very fine energy grid refinement at low energies, where fast changes of cross-section data play a role (cf. Fig. 11c of Balança & Feautrier 1998).

A further step of our analysis has been the evaluation of the polarization degree in the same approximation but under local

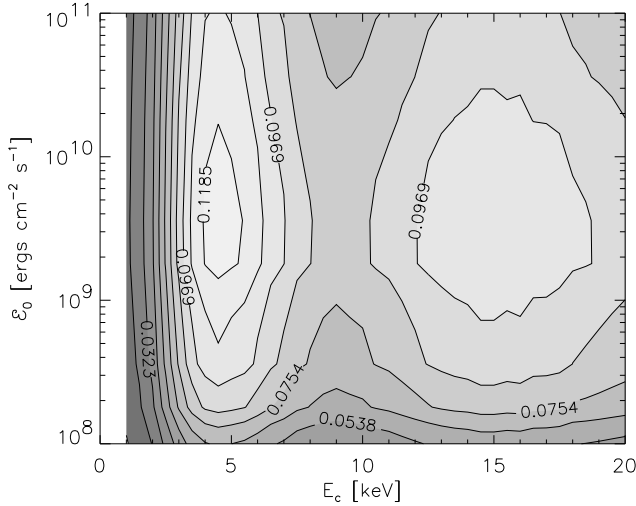


Fig. 7. Same as Fig. 6; here calculated with correct densities of the background electrons (and protons) and modified mean intensities of the radiation field.

physical conditions calculated using the correct solution of the unpolarized radiation transfer (see Sect. 3). An increase of the mean radiation intensity and higher depolarization due to increased ionization degree lead to a significant decrease of the polarization degree by more than one order of magnitude (see Fig. 7). The expected polarization degree is very sensitive to $nlj \rightarrow nl \pm 1j'$ depolarizing transitions between fine structure levels of the same shell caused by background perturbers. The results of this section show that the line polarization is in fact smaller than the previously reported calculations, even if we use the not fully correct approximation (2) for the energy distribution of the beam at the H α core-forming layer.

7. Polarized radiation transfer solution

A self-consistent NLTE solution of the polarized transfer may provide additional information about the polarization degree of the H α line and the effect of the proton beam. In contrast to the results of the previous section, it also provides complete emergent intensity and fractional Q/I polarization profiles. In this section, a short description of the polarized transfer solution is contained. It is beyond the scope of this paper to review the complex problem of self-consistent modeling of the polarized transfer in hydrogen lines and thus we limit our explanation to a few notes about the method. The detailed description of this problem is a subject of other papers (Štěpán 2006, 2007, in preparation).

It is advantageous to describe the polarized radiation field by means of the so-called Stokes vector $\mathbf{S}(\nu, \mathbf{\Omega}) = (I, Q, U, V)^T(\nu, \mathbf{\Omega})$, in which I is the specific intensity, Q and U correspond to the linear polarization parameters with respect to two axes, and V stands for the circular polarization. We limit our analysis to the cylindrically symmetric problem where the natural choice of the reference frame leads to a reduction of the Stokes vector to only two nonvanishing parameters, $\mathbf{S}(\nu, \mathbf{\Omega}) = (I, Q)^T(\nu, \mathbf{\Omega})$, while U and V are identically zero. Stokes parameters are computed from the radiation transfer equation (RTE) formally identical to the unpolarized transfer case (all depen-

dences on the radiation frequency ν and direction of propagation $\mathbf{\Omega}$ are suppressed):

$$\frac{d\mathbf{S}}{ds} = \boldsymbol{\epsilon} - (\boldsymbol{\eta} - \boldsymbol{\eta}_s)\mathbf{S}. \quad (17)$$

The 2-component vector $\boldsymbol{\epsilon}$ stands for the spontaneous emission in Stokes parameters, $\boldsymbol{\eta}$ is the 2×2 symmetry matrix of the absorption, and $\boldsymbol{\eta}_s$ matrix stands for the stimulated emission. Explicit forms of these quantities can be found in Landi Degl'Innocenti (1984). For the purposes of this paper, it is only important to notice that values of these quantities can be calculated directly from the atomic density matrix coefficients ρ_{nlj}^k . In the solar chromosphere, nonlocal coupling of atomic states between different points due to radiation is strong. Therefore we have to solve the nonlinear system of RTE (17) together with ESE (8) at every point of the atmosphere. This so-called NLTE problem of the 2nd kind (Landi Degl'Innocenti 1987) can be solved numerically using efficient iterative NLTE solvers.

We have used our new multigrid technique that calculates the Stokes profiles for a given temperature and density structure of the atmosphere for an arbitrary line overlapping, and the CRD approximation. This method uses the accelerated lambda iteration technique applied to polarized radiation together with the multigrid acceleration technique (cf. Fabiani Bendicho et al. 1997), which improves the convergence rate from $O(N^{3/2})$ to $O(N)$, where N is the number of spatial discretization points in the atmosphere). The formal solver of our method is based on the short characteristics approach (Olson & Kunasz 1987) with the parabolic interpolation of the source function.

The effect of stimulated emission is taken into account as well as the continuum opacity and emissivity. In the present calculations, we have restricted our solution to the first three-principal levels of the hydrogen atom and the transfer has been solved in three spectral lines, i.e., $L\alpha$, $L\beta$, and H α . A 50-point quadrature in frequency for each line and a 14-point quadrature for ray directions has been applied.

Finally, one simplification of our approach should be mentioned. While in common situations the density matrix is treated as independent of atomic velocity, this is not the case for anisotropic charge exchange interaction. In this case, there is a systematic Doppler shift in emission dependent on the direction of observations (Canfield & Chang 1985; Fang et al. 1995). This effect is dominant in the $L\alpha$ and $L\beta$ lines, while the H α line profile is not much affected. In our approximation we do not take into account any Doppler shifts and assume charge exchange to be symmetric with respect to the center of the line. This approximation could lead to a slight overestimation of the impact polarization effect on the H α line.

8. Results & discussion

Particular results of the H α polarization in the approximation neglecting polarized transfer have been presented in Sect. 6. Using our multigrid method, in Sect. 7 we have solved the self-consistent NLTE transfer problem of the 2nd kind for a grid of atmospheres based on F1 and VAL F models affected by proton beams of different fluxes and energy distributions.

Figs. 8 and 9 show the theoretical emergent linear polarization profiles Q/I of the H α line for the F1 and VAL F models respectively. The intensity I -profiles (not shown) are similar to the profiles plotted in Fig. 4, although the intensity in the line core and near wings is overestimated by factor of approximately

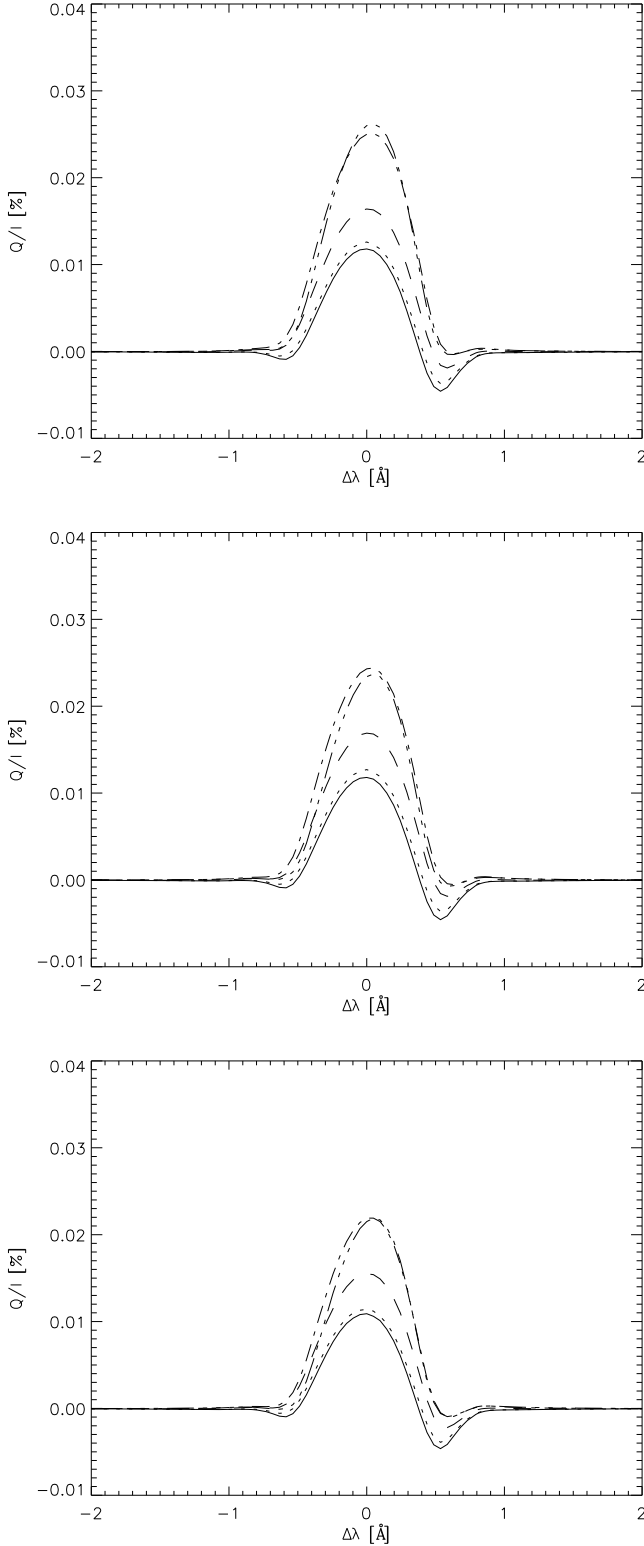


Fig. 8. Emergent fractional linear polarization Q/I profiles computed close to limb ($\mu = 0.11$) for the F1 model and different beam energy distributions: $\delta = 3$ (upper), $\delta = 4$ (middle), and $\delta = 5$ (lower). The different lines correspond to the same beam fluxes as in Fig. 2. All the calculations have been done for $E_c = 150$ keV.

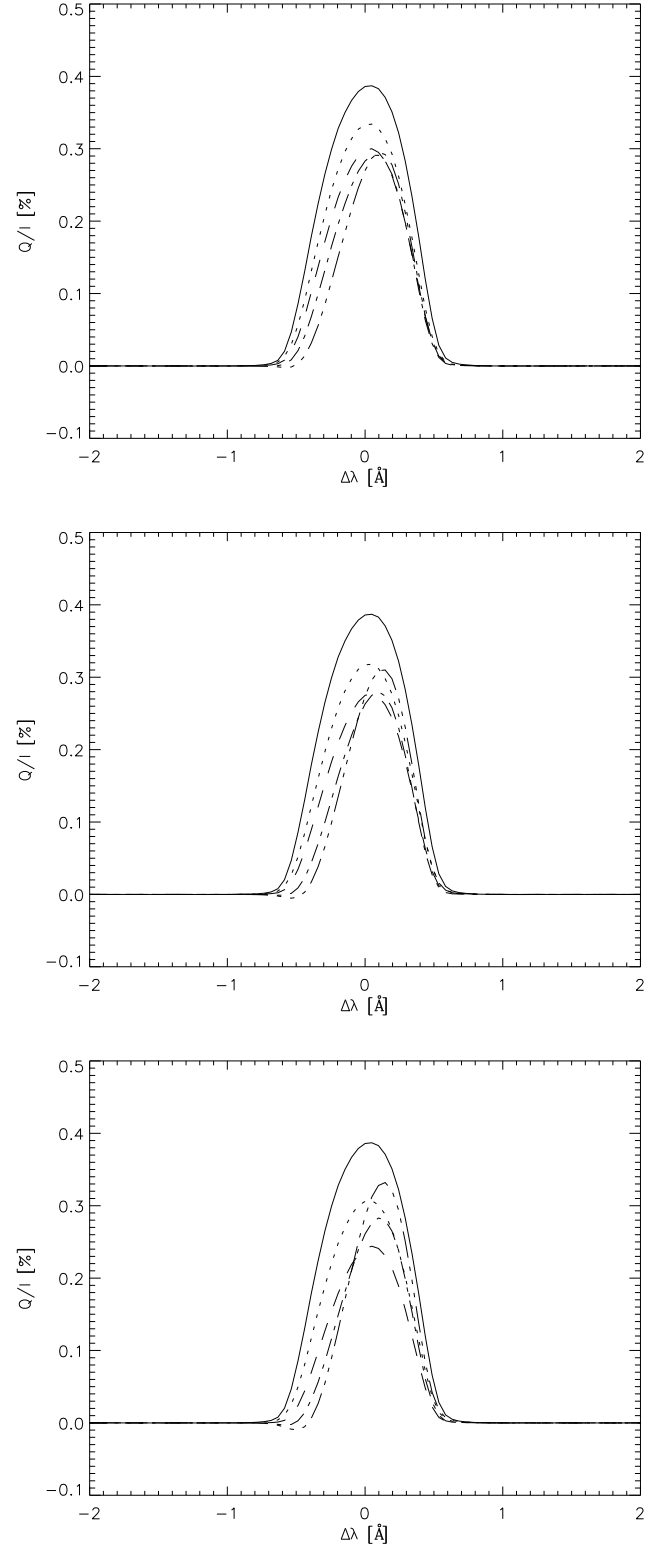


Fig. 9. Same as Fig. 8; here for the VAL F model.

different collisional rates used in both calculations and because the polarized solution was restricted to three-principal levels of the hydrogen atom. However, neglecting the upper level should not affect the emergent polarization profile much. In our notation, a positive sign in Q/I plots means the tangential direction of polarization, while a negative sign is the radial one. Because

1.3–1.5. These differences between intensity profiles are due to

of the symmetry reasons the highest fractional polarization is expected at the limb ($\mu = 0$) and the degree of polarization decreases to zero at the disk center ($\mu = 1$).

The resonance polarization of the H α line in thermal atmosphere (no beams) shows a small tangential polarization of degree 0.01 % for F1 and 0.4 % for VAL F. This shows the dominant role of resonance polarization due to scattering over the impact polarization by the proton beam. The increase of tangential polarization in the F1 model with the beam flux shows the completely negligible effect of the impact polarization in comparison to other effects: the variation of the polarization is driven mainly by shifts of the optical depth scale due to higher ionization degree, which can lead to an increase of the resonance scattering effect on polarization. Another effect is the increase of radiation intensity due to non-thermal excitation in the lower chromosphere layers and an increase of the density of background colliders. All these effects compete in the formation of these small fractional polarizations. The impact polarization contributes by only a small fraction to the total polarization degree in all the studied cases, as was expected from Fig. 7.

Contrary to the conclusions of Vogt et al. (2001), the variation of spectral index δ does not affect the emergent polarization degree much. This is because of the negligible impact polarization effect and because the number of low energy protons in the H α formation layers is similar across the δ values – the initial difference in energy distribution of lower energy protons is quickly lost at depths $E_N \approx E_c$. An effect that could play a role is the variation of E_c energy. The energy distribution of the beam of protons is sensitive to the chromospheric depth parametrized by E_N (see Sect. 2). One expects that a fine tuning of E_c with the energy necessary to reach the H α -forming layers can lead to a more significant effect of impact polarization. We have calculated the dependence of the line center polarization on E_c for a wide range of cut-off energies. The results can be found in Figs. 10 and 11. It is easy to find the effect of impact polarization that emerges at cut-off energies comparable to the energy necessary to reach the H α -forming layer. This effect is seen as a *decrease* in the total polarization degree (i.e., increase of radial atomic polarization due to impacts that has an opposite orientation than the tangential polarization formed preferentially by scattering). In the F1 model, the thermal case of 0.01 % polarization is increased as protons have enough energy to change the structure of the atmosphere at H α formation levels. The effect of impact polarization is seen at about 150 keV when the density of protons is high enough to decrease the dominant tangential polarization. Further increase of E_c again leads to a negligible number of protons with small energies at the H α formation layer. Similar effects can be seen in the VAL F case, where the resonance polarization scattering effect is much stronger. The total number of thermal perturbors is always lower than in the F1 case, but high enough to decrease the thermal atmosphere polarization of 0.4 % even for a small energy cut-off. The impact polarization is best seen at energies around 200 keV: in this cooler model the total column mass above $\tau_{H\alpha} = 1$ is higher than in the F1 case. In any case the emergent linear polarization is low, below the stated 5 % value, and it is even possible to expect a decrease of the total linear polarization due to proton impacts.

9. Conclusions

The purpose of this paper was to verify whether the anisotropic excitation of the $n = 3$ level of hydrogen caused by proton beams can lead to H α line polarization and what degree of polarization can be expected. In our considerations, we have chosen a uni-

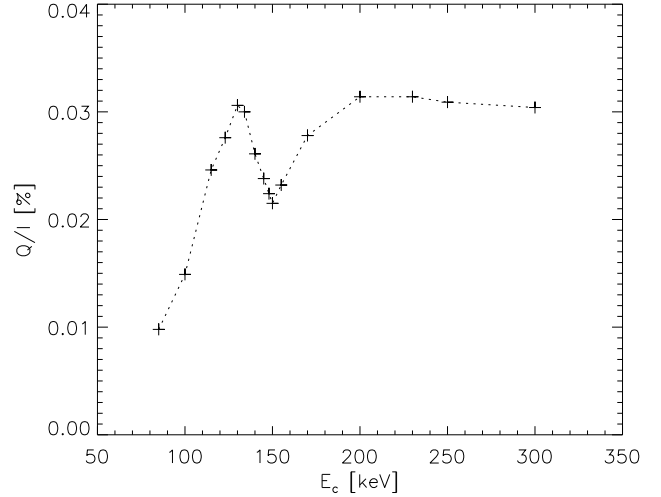


Fig. 10. H α line center polarization as a function of a lower energy cut-off E_c at the injection site. The atmosphere model F1, beam flux $\mathcal{E}_0 = 10^{11} \text{ erg cm}^{-2} \text{ s}^{-1}$, $\delta = 5$. The E_c value has been varied in the interval 85–300 keV.

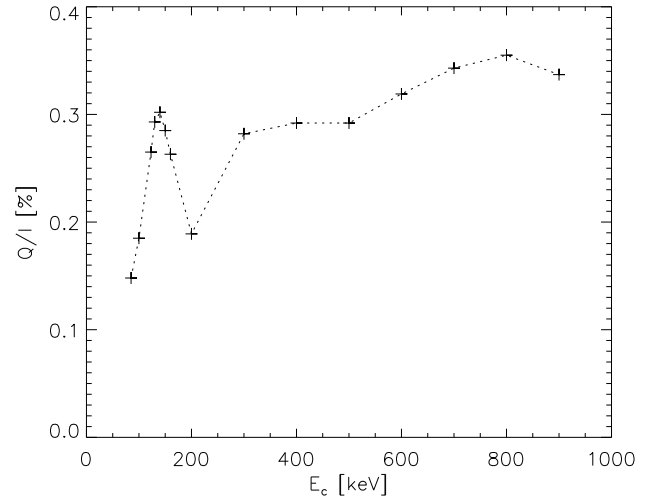


Fig. 11. Same as Fig. 10; here for the chromosphere model VAL F and the E_c energy range 85–900 keV.

rectional vertical beam with an initial power-law energy distribution at the chromosphere injection site, which is not deflected by collisions with constituents of the chromosphere although it is decelerated. For this extremely anisotropic beam we have calculated new chromosphere conditions with a wide range of beam parameters. For all the calculated models we have found the polarization degree well below the values reported in the past. Furthermore, the theoretical polarization degree is mainly caused by resonance scattering.

The absence of impact polarization is consistent with measurements of Bianda et al. (2005), although their conclusions about the beam isotropization are not necessary for explanation of the missing polarization. In fact, a sufficient number of unidirectional low-energy protons at the H α -forming layer cannot be achieved for beams with initial power-law distributions. Although the proton beam may significantly affect the line intensity profile, impact atomic polarization is destroyed by colli-

sions with background electrons and protons and by the strong radiation field. The density of background perturbers is actually higher than that calculated in previous works. In addition, the beam energy distribution at the line formation layers cannot be approximated by a power-law distribution and the effect of a steep increase of fractional polarization with spectral index δ is not observed. Therefore we believe that the polarization occasionally measured (i.e., by some authors) has another source than impacts by proton beams.

Low impact polarization of the H α line by proton beams in solar flares does not seem to be a good candidate for straightforward proton beam diagnostics, at least if most of the usual initial distributions of proton beam energies are considered. It is possible to imagine different initial energy distributions of the same energy flux with very narrow band of energies, which preferentially excite the hydrogen at low energies and in the H α -forming layers. However, the question remains if such a distribution is physically possible and if it can lead to measurable impact polarization.

Recent spectropolarimetric measurements of an M6.3 flare performed by Xu et al. (2005b) indicate the presence of both radial and tangential polarization of the H α line and radial polarization of the H β line at the edges of flare kernels. The process that is believed to play a significant role is the effect of return currents (Karlický & Hénoux 2002). Investigation of this phenomenon remains the subject of further observational and theoretical research.

Acknowledgements. We are indebted to Jana Kašparová for providing her MALI code, for her careful reading of the manuscript, and for her many useful comments. We thank Dr. C. Balança for providing us with his close-coupling data of proton–hydrogen cross-sections. We are grateful to Dr. J.-C. Hénoux and Dr. V. Bommier for clarifying discussions and Dr. E. Vogt for providing us with the radiation transfer code used in his calculations of electron and proton densities in the chromosphere. J.Š. acknowledges the support of the French government during his stay at Paris Observatory – Meudon in the frame of a co-tutelle. He also acknowledges the staff of the LERMA laboratory in Meudon and the Solar Department in Ondřejov for their support and kind hospitality. This work was partially supported by the Grant A3003203 of GA AV ČR.

References

- Aboudarham, J., Berrington, K., Callaway, J., et al. 1992, A&A, 262, 302
 Balança, C. & Feautrier, N. 1998, A&A, 334, 1136
 Bianda, M., Benz, A. O., Stenflo, J. O., Küveler, G., & Ramelli, R. 2005, A&A, 434, 1183
 Bommier, V. 1980, A&A, 87, 109
 Bommier, V., Leroy, J. L., & Sahal-Bréchet, S. 1986a, A&A, 156, 79
 Bommier, V., Leroy, J. L., & Sahal-Bréchet, S. 1986b, A&A, 156, 90
 Bommier, V. & Sahal-Bréchet, S. 1982, Sol. Phys., 78, 157
 Bommier, V. & Sahal-Bréchet, S. 1991, Ann. Phys. Fr., 16, 555
 Brosius, J. W., Robinson, R. D., & Maran, S. P. 1995, ApJ, 441, 385
 Brosius, J. W. & Woodgate, B. E. 1999, ApJ, 514, 430
 Brown, J. C. 1971, Sol. Phys., 18, 489
 Brown, J. C., Karlický, M., MacKinnon, A. L., & van den Oord, G. H. J. 1990, ApJS, 73, 343
 Canfield, R. C. & Chang, C.-R. 1985, ApJ, 295, 275
 Doschek, G. A., Mariska, J. T., & Sakao, T. 1996, ApJ, 459, 823
 Emslie, A. G. 1978, ApJ, 224, 241
 Fabiani Bendicho, P., Trujillo Bueno, J., & Auer, L. 1997, A&A, 324, 161
 Fang, C., Feautrier, N., & Hénoux, J.-C. 1995, A&A, 297, 854
 Fano, U. 1957, Rev. Mod. Phys., 29, 74
 Frost, K. J. 1969, ApJ, 158, L159
 Hénoux, J.-C. & Chambe, G. 1990, Journal of Quantitative Spectroscopy and Radiative Transfer, 44, 193
 Hénoux, J.-C., Chambe, G., Smith, D., et al. 1990, ApJS, 73, 303
 Hénoux, J.-C., Fang, C., & Gan, W. Q. 1993, A&A, 274, 923
 Karlický, M. & Hénoux, J.-C. 2002, A&A, 383, 713
 Kašparová, J. & Heinzel, P. 2002, A&A, 382, 688
 Korchak, A. A. 1967, Soviet Astronomy, 11, 258
 Landi Degl'Innocenti, E. 1982, Sol. Phys., 79, 291
 Landi Degl'Innocenti, E. 1984, Sol. Phys., 91, 1
 Landi Degl'Innocenti, E. 1987, in Numerical radiative transfer, ed. W. Kalkofen (Cambridge: Cambridge University Press), 265–278
 Machado, M. E., Avrett, E. H., Vernazza, J. E., & Noyes, R. W. 1980, ApJ, 242, 336
 Olson, G. L. & Kunasz, P. B. 1987, J. Quant. Spec. Radiat. Transf., 38, 325
 Orrall, F. Q. & Zirker, J. B. 1976, ApJ, 208, 618
 Sahal-Bréchet, S. 1977, ApJ, 213, 887
 Sahal-Bréchet, S., Vogt, E., Thoraval, S., & Diedhiou, I. 1996, A&A, 309, 317
 Štěpán, J. 2006, in proceedings of the 4th Solar Polarization Workshop, ed. R. Casini (ASP Conf. Series, in press (astro-ph/0611112))
 Vernazza, J. E., Avrett, E. H., & Loeser, R. 1981, ApJS, 45, 635
 Vogt, E. & Hénoux, J.-C. 1996, Sol. Phys., 164, 345
 Vogt, E., Sahal-Bréchet, S., & Bommier, V. 2001, A&A, 374, 1127
 Vogt, E., Sahal-Bréchet, S., & Hénoux, J.-C. 1997, A&A, 324, 1211
 Xu, Z., Fang, C., & Gan, W.-Q. 2005a, Chinese Journal of Astronomy and Astrophysics, 5, 519
 Xu, Z., Hénoux, J.-C., Chambe, G., Karlický, M., & Fang, C. 2005b, ApJ, 631, 618
 Zhao, X., Fang, C., & Hénoux, J.-C. 1998, A&A, 330, 351